

Isotopic composition of H₂ from wood burning: Dependency on combustion efficiency, moisture content, and δD of local precipitation

Thomas Röckmann,¹ Catalina X. Gómez Álvarez,¹ Sylvia Walter,¹ Carina van der Veen,¹ Adam G. Wollny,² Sachin S. Gunthe,² Günther Helas,² Ulrich Pöschl,² Frank Keppler,² Markus Greule,² and Willi A. Brand³

Received 11 September 2009; revised 15 March 2010; accepted 6 April 2010; published 15 September 2010.

[1] Differences in isotopic composition between the various sources of H₂ are large, but only a few measurements have been carried out to constrain them. Two conflicting values have been published for H₂ from biomass burning. Both rely on the assumption that the isotopic composition of H₂ should scale with the isotopic composition of the precipitation at the location where the biomass grew. Here we test this hypothesis using 18 wood samples collected from various locations around the globe. The sample locations cover a range of δD content of H₂ in precipitation, from below -120‰ in Siberia and Canada to -15‰ in Zimbabwe. The results confirm the predicted dependence of the H₂ isotopic composition on the precipitation in the sampling region. The water content itself is found to at most slightly affect the results. Furthermore, δD of H₂ depends strongly on combustion efficiency. Thus, the isotopic composition of H₂ from biomass burning shows a strong variability around the globe and between different stages of a fire. It is suggested that, rather than a global bulk number, global models that attempt to reproduce the spatial and temporal distribution of δD in H₂ should incorporate explicitly the variability of $\delta D(\text{H}_2)$ from biomass burning on δD in precipitation.

Citation: Röckmann, T., et al. (2010), Isotopic composition of H₂ from wood burning: Dependency on combustion efficiency, moisture content, and δD of local precipitation, *J. Geophys. Res.*, 115, D17308, doi:10.1029/2009JD013188.

1. Introduction

[2] Compared to many other atmospheric trace species, the atmospheric cycle of molecular hydrogen (H₂) has been scarcely investigated. Only in recent years has interest in H₂ increased, which is related to its potential use as a future energy carrier and the expected increase of H₂ in the atmosphere due to leakage in the production, storage, distribution, and use of H₂ [Feck et al., 2008; Schultz et al., 2003; Tromp et al., 2003; Warwick et al., 2004]. To assess the impact of a future hydrogen economy, it is important to understand its atmospheric cycle in more detail before a potentially drastic anthropogenic change takes place. The present understanding of the atmospheric H₂ budget is shown in Table 1. The budget from Ehhalt and Rohrer [2009] results from a critical review of the existing literature and the reader is referred there for an excellent summary of other individual budget studies. The main sources of H₂ are combustion processes (fossil fuel combustion and biomass burning) and atmospheric

oxidation sources (from CH₄ and volatile organic compounds, VOCs), with smaller contributions from the oceans and terrestrial nitrogen fixation. H₂ is removed from the atmosphere by deposition to the soil and oxidation by OH. However, all values for source and sink strengths have relatively large errors (Table 1).

[3] One possibility to get further insight into the relative strengths of individual sources and sinks is by measuring the isotopic composition [Breninkmeijer et al., 2003; Johnson et al., 2002]. Different sources and sinks produce H₂ with different isotopic composition because of the slightly different physical and chemical properties of HH and HD, which depend on molecular mass. For H₂, the associated isotope effects are particularly large, since HH and HD differ in mass by 50%. In fact, the D/H ratio of H₂ emitted from various sources to the atmosphere varies by a factor of 2. The D content is quantified as $\delta D = [D/H]_{SA}/[D/H]_{ST} - 1$, where $[D/H]_{ST}$ denotes the D/H ratio of the international standard material Vienna Standard Mean Ocean Water (VSMOW). For H₂, only a few experimental studies have investigated the isotope signatures in detail; the present knowledge on the isotopic composition is shown in Table 1. Much of the isotope information is based on the seminal paper by Gerst and Quay [2001], who presented the first thorough approach for constructing a global δD budget for H₂.

¹Institute for Marine and Atmospheric Research Utrecht, Utrecht University, Utrecht, Netherlands.

²Max Planck Institute for Chemistry, Mainz, Germany.

³Max Planck Institute for Biogeochemistry, Jena, Germany.

Table 1. Sources and Sinks of H_2 and Their Isotopic Signatures

	Strength (Tg/yr)		Isotopic Signature
	<i>Novelli et al.</i> [1999]	<i>Ehhalt and Rohrer</i> [2009]	
<i>Sources</i> ^a			
Fossil fuel combustion	15 ± 10	11 ± 4	-196 ^c
Biomass burning	16 ± 5	15 ± 6	-290 ^c
CH ₄ oxidation	26 ± 9	23 ± 8	-162 ^d
VOC oxidation	14 ± 7	18 ± 7	-162 ^d
Ocean N fixation	3 ± 2	6 ± 3	-628 ^d
Land N fixation	3 ± 1	3 ± 2	-628 ^d
Total sources	77 ± 16	76 ± 14	
<i>Sinks</i> ^b			
Soil deposition	56 ± 41	60 ⁺³⁰ ₋₂₀	0.943 ^c
Reaction with OH	19 ± 5	19 ± 5	0.568 ^c
Total sinks	19 ± 5	79 ⁺³⁰ ₋₂₀	

^aIsotopic signatures for sources are listed in ‰.

^bIsotopic signatures of sinks are listed as fractionation factors, i.e., the ratio of the removal rates of HD and H₂.

^cFrom *Gerst and Quay* [2001].

^dFrom *Price et al.* [2007]. Signatures for oxidation sources were determined from the budget.

^eFrom *Sander et al.* [2006].

[4] New analytical techniques have significantly simplified isotope analysis on H₂ [*Rahn et al.*, 2002b; *Rhee et al.*, 2004]; as a result, an increasing number of measurements are now becoming available to study both the isotope composition of various H₂ sources and its variations in the atmosphere [*Feilberg et al.*, 2007; *Rahn et al.*, 2002a, 2003; *Rhee et al.*, 2006a, 2006b, 2008; *Rice et al.*, 2010; *Röckmann et al.*, 2003, 2010; *Vollmer et al.*, 2010]. In the European project EUROHYDROS, annual cycles of H₂ concentration and δD at six stations worldwide have been recently determined (A. Batenburg et al., manuscript in preparation).

[5] Isotope data are now also being included in model studies to constrain the global H₂ budget [*Pieterse et al.*, 2009; *Price et al.*, 2007]. It is clear that the results of such studies can only be as good as the data they use as input, and therefore, an intensive approach is required to better define and understand the isotope signatures of the source and sink processes.

[6] In this study, we focus on the H₂ produced from biomass burning. The value in Table 1 of $\delta D = -290\%$ is taken from the only available direct combustion experiments [*Gerst and Quay*, 2001]. This number is based on the analysis of a total of six air samples from two experimental fires carried out with pine needles and pine branches in Montana. The results were then extrapolated to the global scale by applying the derived fractionation factor between biomass and H₂ from biomass burning to a global average δD content of biomass. *Rhee et al.* [2006b] presented an indirect top-down estimate of $\delta D = -90\%$ as global average source signature of H₂ from biomass burning on the basis of analysis of air samples collected near the tropical tropopause above biomass-burning regions. Note that in these samples a biomass burning signal could not be observed directly in the H₂ mixing ratio; rather, the biomass burning source was identified by a CO elevation, and the H₂/CO emission ratio was used to determine the likely contribution of H₂ from biomass burning. The absence of a H₂ combustion peak was interpreted by postulating an interference of a simultaneous

soil sink signal that cancels out the H₂ peak. Thus, this estimate is rather indirect and involves numerous assumptions, but the derived δ value is much higher than that obtained from the direct fire samples.

[7] For both studies, the calculation of the global average δD value for H₂ from biomass burning is based on the assumption that the signature should scale with the δD in precipitation that plants use as their hydrogen source [*Yapp and Epstein*, 1982]. Although this assumption is reasonable, it has never been experimentally verified. To test this hypothesis, we carried out combustion experiments with wood samples from various regions around the globe. We note here at the outset that in natural fires it is often not the wood but the foliage and grass that is burning; the stems and larger branches of trees often are left after the fire. Table 4 from *Ehhalt and Rohrer* [2009] shows that H₂ generated from biomass burning is a mix of numerous different fuel types. For the purpose of this study, we decided to use wood samples having an estimated age of at least 5 years. Analysis of short-lived biomass may bias the results due to, e.g., seasonal changes in δD of precipitation, dependency on the growth season, and evaporative enrichments in the leaves [*Roden and Ehleringer*, 2000]. Using wood samples means that seasonal and short interannual effects should average out. This approach is not motivated by the idea to derive a revised global average for $\delta D(H_2)$ from biomass burning, but it is well suited for our objective.

2. Experimental

[8] Table 2 lists the origin and specification of 18 wood samples from 10 countries that were collected from different regions around the globe. All samples were collected from a typical tree species from the respective region. Most samples were pieces of branches between 3 and 8 cm in diameter; the samples from Siberia, Chile, and Sydney were pieces of a trunk. Samples were cut into easily combustible small pieces ($\sim 1.5 \times 1.5 \times 8$ cm), and 300–500 g of each was combusted in an experimental combustion chamber contained in a trailer at the Max Planck Institute for Chemistry in Mainz, Germany [*Lobert et al.*, 1990].

[9] A propane flame is used to ignite the wood. Additionally a warm air blower is used in some cases when needed. Once the fire has reached a self-sustaining stage, these accessories are removed and several air samples are collected until the end of the smoldering stage. In rare cases, especially when the wood is not dried before the experiment, reignition is necessary; this is done during times when no air samples are taken. The combustion efficiency is monitored online with CO and CO₂ Heraeus BINOS sensors. These measure, via infrared absorption, mixing ratios for the two gases to a sensitivity of a few ppm, at a noise level of 1 ppm. Calibrations are done using a standard gas [*Lobert et al.*, 1991]. All online data were recorded with a V25 data acquisition system (developed at the Max-Planck Institute for Chemistry, Mainz), which also logs outside temperature and moisture. Measurements of temperature in the combustion zone were not available.

[10] Air is sampled for isotope analysis from a chimney above the trailer, which is equipped with several valves for sampling [*Lobert et al.*, 1991]. To ensure steady updraft

Table 2. Overview of Samples Burned^a

Country	Sample Identification	Number of Air Samples	Location	Altitude ^b	Location	Species
Australia	S.4	3	33°S, 151°E	60	Sydney	<i>Eucalyptus racemosa</i>
	S.1	3	27°S, 153°E	40	Brisbane	Unknown wood
	S.22	10	27°S, 153°E	40	Brisbane	Unknown wood
China	S.2	3	40°N, 117°E	200	Shangdianzi	Plum (unspecified)
	S.12	6		200		Corn (unspecified)
Chile	S. 11	8	38°S, 72°W	335	Victoria valley	Oak
	S.3	3	39°S, 71°W	1000	Curarrehue	Oak
	S.9 (rep.)	5		1000	Cordillera	
	S.5	3	49°N, 123°W	80	Pacific Spirit	Spruce
Canada	S.15, wet	7	49°N, 126°W	400	Chibougamau, Québec	Unknown wood
	S.16, dry	9		400		
	S.17, dry	10	49°N, 74°W	0	Estevan Pt., BC	Unknown wood
	S.18, wet	8		0		
	S.23	14	54°N, 105°W	530	East Trout Lake, Sask.	Unknown wood
Finland	S.6	3	60°N, 24°E	115	Loppi	<i>Pinus sylvestris</i>
	S.13 (rep.)	7		115		
Nepal	S.7, wet	5	33°N, 80°E	2000	Himalaya	Unknown wood
	S.8, dry	5		2000		
Russia	S.14	8	60°N, 90°E	47	Zotino, Siberia	<i>Pinus sylvestris</i>
	S.21 (rep)	8		47		
Puerto Rico	S.10	4	18°N, 66°W	250		Unknown wood
Zimbabwe	S.19	10	18°S, 31°E	1000		<i>Brachystegia</i> genus
Namibia	S.20	10	19°S, 30°E	1100	Etosha National Park	<i>Colophospermum mopane</i>
10 countries	23 fires	152				

^arep, repetition of the same sample.

^bApproximate altitude as used in the OIPC (see Table 3), meters above sea level.

conditions, a fan was placed 1.5 m above the valves in the chimney. One of the valves was connected to a 1.5 or 2 L volume evacuated glass or stainless steel flask via a DRIERITE™ drying trap. Sampling was performed by simply opening and closing the canister valve.

[11] At times determined to be representative of the different combustion stages, the valve on the evacuated flask was opened for about 30 s and combustion gases were collected. The number of samples taken from a single fire ranged from 3 in the beginning of the experiment to more than 10 as improvements in operational procedures and flask availability were achieved. Besides the flasks with combustion gas samples, we took samples of the background air on each sampling day to measure ambient H_2 concentration and δD .

[12] The flasks containing the combustion air samples were analyzed in the isotope laboratory of the Institute of Marine and Atmospheric Research Utrecht (IMAU). Isotope composition (δD) and mixing ratio of the H_2 were determined with a system based on isotope monitoring ratio mass spectrometry (IRMS), in which the D/H ratio in a sample is measured relative to that of a reference air cylinder with known isotopic composition and mixing ratio and the δD value is calculated on the Vienna Standard Mean Ocean Water (VSMOW) scale.

[13] The analytical system is described in detail in the work of Rhee *et al.* [2004]. Briefly, an air or reference air sample is admitted via a DRIERITE™ trap to the sample volume of the system, where its pressure is determined as an indicator of the total amount of air. It is then flushed to a cold head of a liquid He compressor cooled to ~ 35 K, where most of the air is condensed except for H_2 , He, and Ne. Those gases pass the cold head trap and are flushed to a preconcentration trap for the collection of H_2 ; the trap consists of a stainless steel tube packed with the 5 Å molecular sieve, cooled to 63 K by immersing the trap into

liquid N_2 and continuously pumping away the N_2 vapor. After being trapped, the H_2 is transferred to the cryofocusing trap, a capillary column packed with molecular sieve 5 Å jacketed in a stainless steel tube. From this trap, the sample is directed over a gas chromatograph for final purification before entering the IRMS system (ThermoFinnigan Delta plus XL) by way of an open split system; using a reduced flow rate of ~ 0.5 nL/min maximizes transfer to the IRMS. Typical peak areas are 7–10 V s for 350 mL air samples with ambient H_2 concentrations of ~ 500 ppb, which corresponds to 175 nL or ~ 7 nmol H_2 . To correct for day-to-day drift in the system, a working reference gas is measured, usually twice per day, and the daily average is used for correction. Calibrations of the δ scale by using mixtures of certified H_2 reference gases of different isotopic compositions show that the scale contraction in our analytical system is very small (no significant scale contraction has been found within the analytical errors).

[14] Bulk δD was determined at the Stable Isotope Laboratory of the Max Planck Institute for Biogeochemistry in Jena (Germany). The method for bulk δD analysis, which uses a high-temperature conversion mass spectrometric technique, closely follows the procedure described for $\delta^{18}O$ determination in bulk material by Brand *et al.* [2009]. Samples are weighed into Ag foil and positioned into an Autosampler (Zero-Blank; Costec, Milan, Italy). Upon actuation, the packets drop into a helium-flushed high-temperature reactor (HTO; Hekatech, Wegberg, Germany) kept at 1450°C. The reactor has an outer SiC tube and an inner tube made from glassy carbon; reversed carrier gas flow between the two tubes ensures that the full helium flux passes through the core of the reactor [Gehre *et al.*, 2004]. In addition, the inner tube is filled with glassy carbon chips up to the highest-temperature zone, where the reaction to CO, H_2 , and carbon plus further unspecified reaction products and residues takes place. From the reactor, the sample

gas passes a fine filter containing NaOH on pumice (Ascarite) and $Mg(ClO_4)_2$ before entering a packed column (5 Å) gas chromatograph at 70°C for separating H_2 and CO. An open split interface [ConFlo III; Werner *et al.*, 1999] provides the connection to a Delta⁺XL stable isotope mass spectrometer (both from Thermo-Fisher Scientific, Bremen, Germany). Analysis of the ion currents at monitoring m/z 3 and 2 yielded the hydrogen isotopic composition. For the primary reference for reporting on the VSMOW scale, we used NBS22 oil with an assigned value of -118.5% . Using this material, a local reference material “PET-J1” (polyethylene, “Uvasol”; Merck, Darmstadt, Germany) was calibrated with a δD value of -80.75% versus VSMOW. Aliquots of these materials were interspersed together with the samples and analyzed in the same sequence. The reported sample results are based on the relative differences to the working reference material results. As a quality control reference, we included one sample of IAEA-CH7 polyethylene (International Atomic Energy Agency, Vienna, Austria) in the daily sequence of measurements. IAEA-CH7 has an assigned value of -100.3% on the VSMOW scale.

[15] δD of the plant methoxyl groups were analyzed as described by Greule *et al.* [2008]. In brief, methoxyl groups of plant material are cleaved off with hydriodic acid (HI) at 130°C in closed reaction vials. Subsequently, a headspace analysis of the gaseous product methyl iodide (CH_3I) is carried out using gas chromatography pyrolysis/combustion IRMS (GC-P/C)-IRMS. This rapid and precise method enables the determination of both $\delta^{13}C$ and δD values of plant methoxyl groups without apparent isotopic discrimination.

3. Results and Discussion

[16] The general characteristics of the combustion experiments, in particular combustion efficiency, are presented in section 3.1. As a by-product, $[H_2]/[CO]$ emission factors were also determined from the combustion experiments and are discussed in section 3.2. The possible influence of moisture in the sample is studied in section 3.3. In section 3.4, the source signatures for each piece of wood are calculated. These are then compared with the δD of the bulk biomass, the δD of methoxyl groups, and the δD of precipitation at the location where the sample was collected.

3.1. Combustion Efficiency

[17] The combustion efficiency characterizes the effectiveness of the combustion and is largely dependent on the availability of oxygen but also on other factors such as combustion temperature. It is determined from the relative mixing ratios of the combustion products carbon monoxide (CO) and carbon dioxide (CO_2). When insufficient O_2 is available, a relatively larger amount of CO is formed, and the combustion is termed inefficient. The efficiency is quantitatively characterized by the ratio $\Delta CO/\Delta CO_2 = (CO_{\text{sample}} - CO_{\text{ambient}})/(CO_2_{\text{sample}} - CO_2_{\text{ambient}})$ [Andreae and Merlet, 2001]. For practical purposes we set $CO_{\text{ambient}} = 0$ ppm and $CO_2_{\text{ambient}} = 360$ ppm. For $\Delta CO/\Delta CO_2 < 8\%$, the combustion process is considered efficient. Higher values indicate inefficient combustion [Andreae and Merlet, 2001]. Note that we did not actively change O_2 levels.

[18] Figure 1a shows CO and CO_2 mixing ratios during a fire of a dried wood sample (S.16). Except for this specific

sample, other samples were not artificially dried before combustion. Ideal burning conditions lead to an undisturbed fire with efficient combustion (low $\Delta CO/\Delta CO_2$) at the beginning of the fire in the flaming stage and inefficient combustion in the smoldering stage ($\Delta CO/\Delta CO_2 > 0.08$). Figure 1b shows the same indicators of combustion efficiency for a piece of the same wood that was not dried and had arrived with high moisture content at our laboratory. This piece of wood was difficult to combust. It was reignited several times during the experiment but the fire never reached a stable flaming stage.

3.2. $[H_2]/[CO]$ Emission Factor and Its Dependence on Combustion Efficiency

[19] Figure 2 shows the measured values for $\Delta[H_2]/\Delta[CO]$, that is, $([H_2]_{\text{sample}} - [H_2]_{\text{ambient}})/(CO_{\text{sample}} - CO_{\text{ambient}})$, for all analyzed samples plotted versus combustion efficiency, where $[H_2]_{\text{ambient}} = 550$ ppb and $[CO]_{\text{ambient}} = 0$ for practical purposes. No clear dependence of the emission factor on combustion efficiency can be detected with the available data, but the large scatter may preclude detection of a relation. However, recent results for H_2 from vehicle exhaust [Vollmer *et al.*, 2010] also have shown that the $[H_2]/[CO]$ emission factor before the three-way catalytic converter does not depend strongly on combustion efficiency as indicated by the setting of the λ sensor, which controls fuel supplied to the motor. When some clear and unexplained outliers are excluded, the average emission factor is 0.16 ± 0.13 mol/mol. This is lower than the range of 0.24–0.52 mol/mol (converted from 0.017–0.037 kg/kg) given by Novelli *et al.* [1999]. We estimated that the determination of the H_2 concentration and thus of the $[H_2]/[CO]$ emission factor may have a maximum bias of $\pm 20\%$ due to difficulties of determining very high H_2 concentrations (1000s of ppm) with our analytical system, which is usually designed to measure atmospheric H_2 levels of 500 ppb only. However, this possible bias cannot be the main cause for the large scatter and the observation that $[H_2]/[CO]$ does not scale with combustion efficiency.

3.3. Dependence of δD on Combustion Efficiency

[20] The correlation between δD and combustion efficiency is shown in Figure 3. Despite the large scatter, one can see that δD decreases with increasing $\Delta CO/\Delta CO_2$. This is qualitatively in line with the findings by Gerst and Quay [2001], who found a difference of 100‰ between flaming (efficient combustion) and smoldering phase for two samples of pine needles and branches (Figure 3). It also agrees qualitatively with the dependence of δD in H_2 from vehicle exhaust on the setting of the λ sensor [Vollmer *et al.*, 2010]. Incomplete combustion leads to higher fractionation between the bulk material (see below) and the H_2 emitted, resulting in observation of isotopically lighter hydrogen. Clearly, however, there is a large scatter in the data, and other factors must also contribute, such as the degree of mixing between background H_2 and combustion H_2 or the different δD of precipitation in the region where the wood grew. As a first indication of the latter, which will be studied in more detail below, the color code in Figure 3 specifies the absolute latitude range of the origin of the wood sample. It is obvious from these raw data that wood from lower latitudes

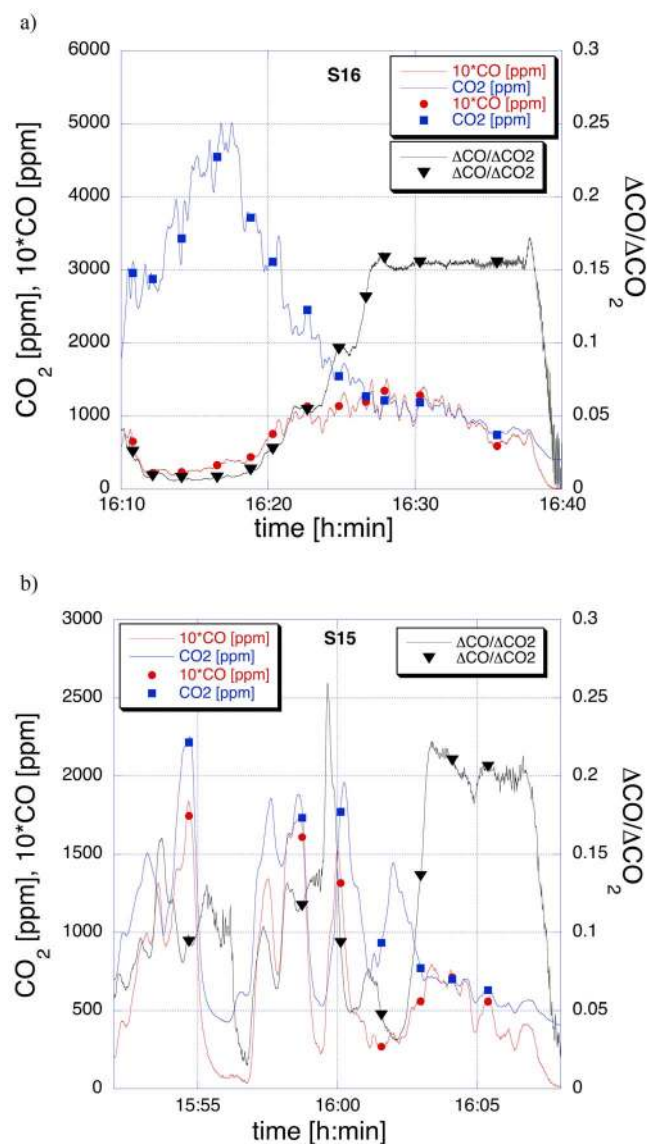


Figure 1. Mixing ratios for CO and CO₂ and combustion efficiency $\Delta CO/\Delta CO_2$ over the course of (a) an undisturbed and (b) a disturbed combustion experiment. Efficient combustion is characterized by $\Delta CO/\Delta CO_2 < 0.08$. The wood for experiment (b) had not been dried before the experiment, and the sample had to be reignited several times. The symbols indicate the times when flask samples for isotope analysis were taken.

liberates H_2 that is generally isotopically heavier than wood from higher latitudes does.

3.4. The Influence of Water Content on δD , a Qualitative Case Study

[21] Molecular hydrogen can be formed from H_2O in the water gas shift reaction, $CO + H_2O \rightarrow CO_2 + H_2$. Therefore, not only the H bound in the biomass but also the water content may be important sources of H_2 in the combustion process and affect the δD values. We tested this in two experimental series: First, we compared results for one dry

and one wet sample of the same species of wood. As shown in Figure 4, the deuterium isotope ratio of the hydrogen released from burning biomass varies strongly with combustion efficiency, as discussed above. The δD results from the two combustion experiments are similar, demonstrating that the water content of the wood does not have a large influence on δD in the H_2 emitted during combustion. The deviating point for the wet sample, located at $\delta D \sim -100\%$ and $\Delta CO/\Delta CO_2 \sim 0.06$, is probably affected by problems with ignition of the wet wood sample. Only partial and highly variable combustion was occurring, which may explain the anomalous results in δD . Omitting this point actually results in the trendlines separating somewhat (Figure 4), but the differences between dry and wet wood are only 20%–30%.

[22] To further investigate the effect of moisture content, we artificially dried in an oven for 1 week at 90°C parts of samples S15 and S18, which arrived in our laboratory with a high moisture content. The dried parts S16 and S17 were extremely dry compared with their untreated counterparts and are “textbook examples” of an undisturbed combustion (see Figure 1, S16), whereas the combustion evolution of the original samples was much more irregular and inefficient (see Figure 1, S15).

[23] Figure 5 shows that for similar combustion efficiencies, the air samples from the “wet” experiment have slightly higher δD values than do the dry samples, and the linear fit lines from the dry samples lie below those from the wet samples. The behavior is thus the opposite of that seen in the experiments described above. Given the large scatter of δD values around the linear fit line within one wood sample, no firm conclusion can be derived from the present experiments. However, at least the water content of the wood does not appear to play a dominant role for the isotopic composition of H_2 produced from biomass burning.

[24] An additional question regarding the influence of water is whether the H_2 could be in thermodynamic equilibrium with the H_2O formed during combustion. Since neither the isotopic composition of the water vapor nor the combustion temperature was measured in our experiments, this cannot be assessed, but it should be investigated in future studies.

3.5. δD Source Signatures

[25] The H_2 measured in the sample is a mixture of background H_2 and H_2 produced from the combustion. In practice, the concentrations in most of the combustion samples are so high that the influence of the background air is not critical. For $\sim 10\%$ of the samples, measured concentrations are in the range 2–5 ppm so the influence of the background air is still $>10\%$. Therefore, the isotopic signature of the pure combustion H_2 was derived from a Keeling plot analysis where the source signature is given by the y axis intercept in a plot of δ versus inverse H_2 concentration. It is necessary to include in this analysis the isotopic composition and concentration of the background air, for which we used the average background determined on the different days. A possible bias may be introduced because this value for background air reflects the composition of the air outside the chamber; it may vary inside the chamber due to the influence of the prior fires. Nevertheless, the low- H_2 concentration samples do actually fit the Keeling

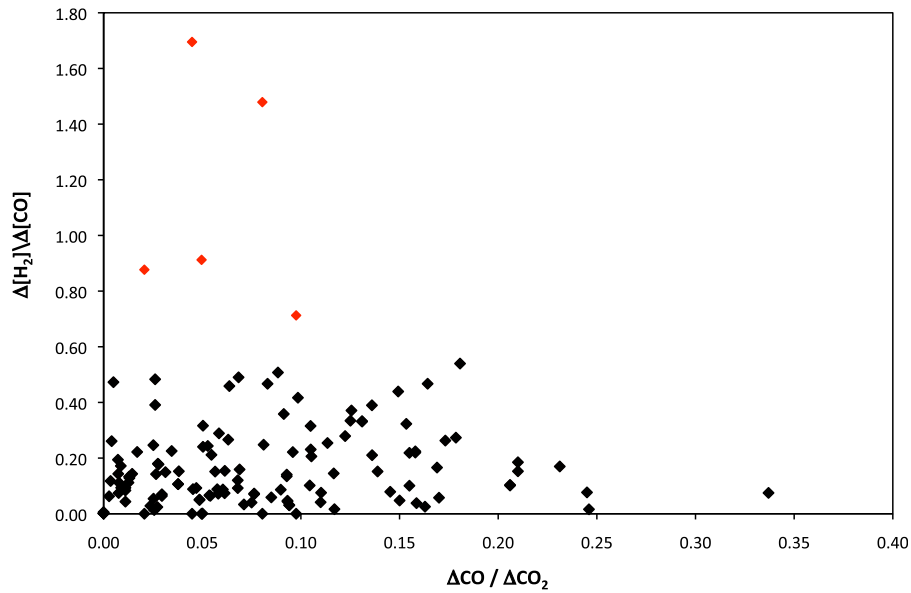


Figure 2. $\Delta[H_2]/\Delta[CO]$ plotted as a function of $\Delta CO/\Delta CO_2$ for all samples. No clear dependence on combustion efficiency is detected. The mean $\Delta[H_2]/\Delta[CO]$ value is 0.16 ± 0.13 without and 0.20 ± 0.24 with the outliers (red). The high amount of scatter is unlikely to be the result of the analytical procedure only.

relation well, and the background correction procedure appears to be valid. For all other samples, the Keeling plot analysis returns δ values that are on average 20‰ lower than simply the averages of the measurements.

[26] The linear fit to the δD versus $1/[H_2]$ correlation of all samples yields an intercept of $\delta D_{source} = -262\text{‰}$. For the subgroup of the efficient ($\Delta CO/\Delta CO_2 < 0.08$) combustion

samples, the intercept is -237‰ ; for the inefficient combustion samples, it is -291‰ . These numbers are of course dependent on the selection of samples. Therefore, we also performed Keeling plot analysis for each combustion experiment individually, when at least two samples from the efficient and inefficient categories were available; the results are shown in Table 3. The average standard deviation on the

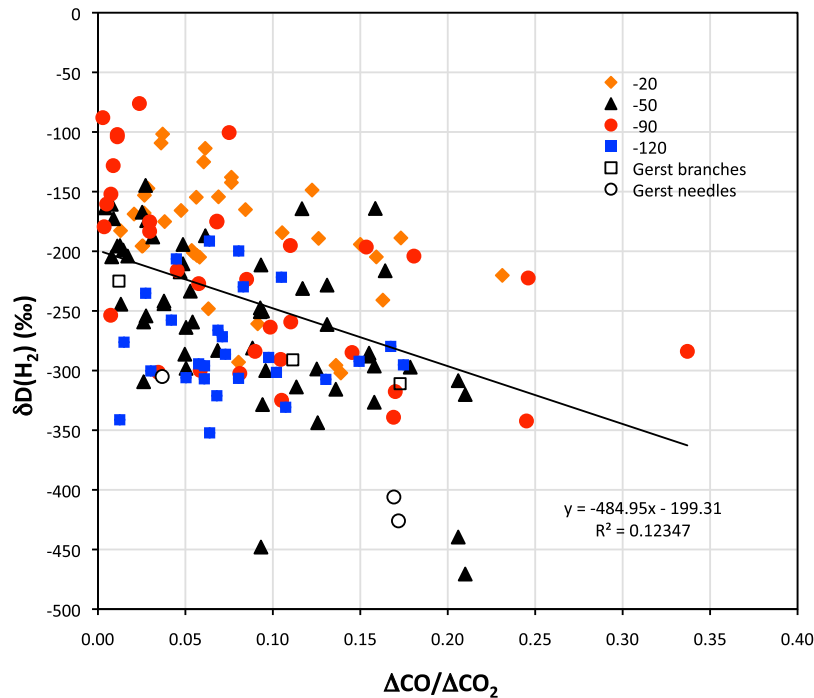


Figure 3. Overview of all results showing the correlation between $\delta D(H_2)$ and $\Delta CO/\Delta CO_2$. Different colours indicate groups of wood samples from locations where δD of precipitation is within $\pm 10\text{‰}$ of the specified value. Open symbols show results of *Gerst and Quay* [2001].

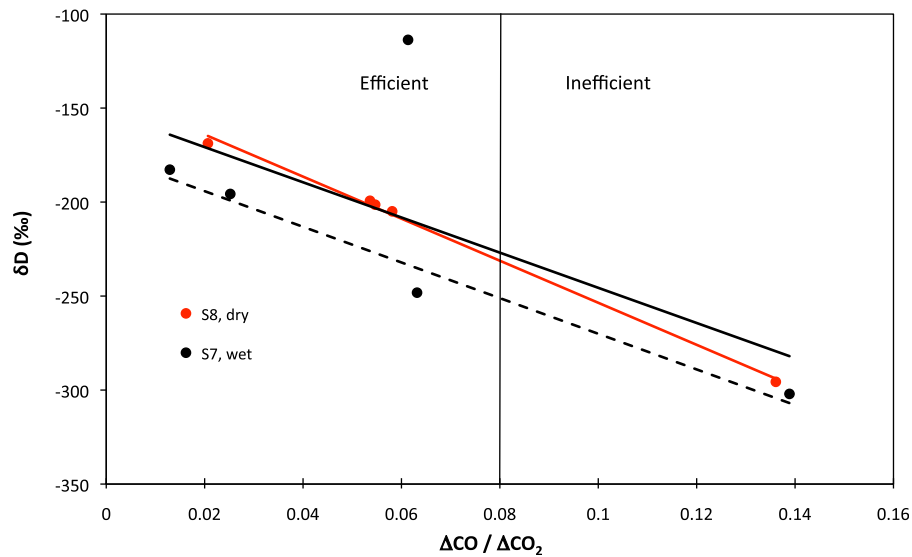


Figure 4. δD and $\delta CO/\delta CO_2$ for two selected wet and dry wood samples. The dashed line shows the linear fit to the data without the outlier (the exceptionally high δD value).

y axis intercept of the Keeling plot for all individual fires is $\pm 27\%$. The average correlation coefficient is $R^2 = 0.89$. For most individual experiments, the source signatures are heavier for the efficient combustions than for the inefficient ones.

3.6. δD of the Bulk Biomass and Methoxyl Groups

[27] Table 3 also shows δD data for the bulk plant material and the methoxyl groups that were determined on the samples. Clearly, the bulk biomass is much more enriched

than the H_2 emitted from biomass burning. The average fractionation factor for all individual fires is $\alpha_{H_2\text{-biomass}} = (\delta_{H_2} + 1) / (\delta_{\text{biomass}} + 1) = 0.85 \pm 0.05$ (1σ), which agrees very well with the fractionation found for pine branches by *Gerst and Quay* [2001]. The slope of the $\delta D_{H_2} - \delta D_{\text{bulk}}$ regression line is 1.02 ± 0.39 . The large uncertainty reflects the considerable scatter and shows that other factors contribute, for example, the different degree of efficient/inefficient samples for the different combustion experiments or variations in mixing ratios but also differences between plant species. Further-

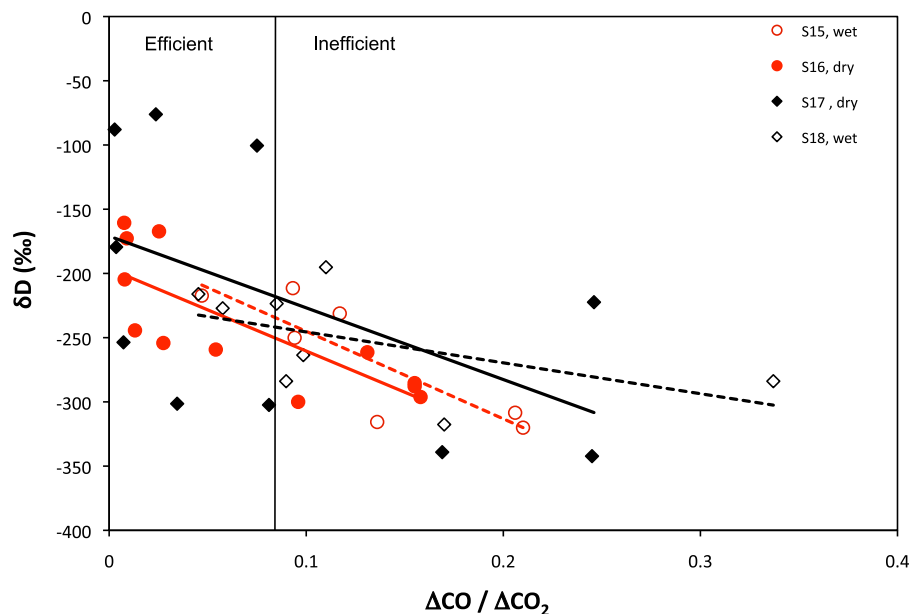


Figure 5. δD of H_2 produced in the combustion of dry (full symbols, solid lines) and wet (open symbols, dashed lines) wood samples as a function of combustion efficiency. Samples S15 and S16 are from the same piece of wood, but sample S16 was thoroughly dried in an oven before combustion. The same is true for samples S17 and S18, S17 being the dried sample.

Table 3. Overview of δD Values in ‰ From the Wood Burning Experiments^a

Sample	Short Name	All	Eff.	Ineff.	Bulk	Methoxyl-	Precip.
S1	Brisbane 1	-212	-204	-217	-82	-250	-21
S2	China	-194		-197	-108	-278	-58
S3	Chile Cordillera 1	-248	-277		-103	-274	-67
S4	Sydney	-179	-149		-67	-187	-23
S5	Pacific Spirit, CA	-231	-206		-108	-303	-90
S6	Loppi Finland	-237		-237	-123	-286	-88
S7	Nepal Fresh	-228	-204		n.m.	n.m.	-61
S8	Nepal Dry	-230	-208		n.m.	n.m.	-61
S9	Chile Cordillera 2	-235	-209		-103	-274	-67
S10	Puerto Rico	-176	-176		-72	-266	-15
S11	Chile Valley	-260	-242	-305	n.m.	-269	-54
S12	China 2	-297	-296	-298	-108	-278	-58
S13	Loppi Finland 2	-325	-295	-379	-123	-286	-88
S14	Zotino 1	-243	-205	-258	-137	-315	-122
S15	Chibougamau Wet	-328		-307	n.m.	n.m.	-89
S16	Chibougamau Dry	-273	-256	-287	-151	n.m.	-89
S17	British Columbia Dry	-311	-260	-351	n.m.	n.m.	-88
S18	British Columbia Wet	-287	-267	-294	-108	n.m.	-88
S19	Zimbabwe	-239	-230		-102	n.m.	-19
S20	Namibia	-167	-155	-194	-82	n.m.	-23
S21	Zotino 2	-309	-315	-295	-72	n.m.	-122
S22	Brisbane 2	-208	-204		-84	-250	-21
S23	East Trout Lake	-302	-295	-319	-155	n.m.	-124
All samples		-250	-231	-287			

^aColumn 3 gives the source signature calculated from all samples. Values for efficient samples only (column 4) and inefficient samples only (column 5) are given if at least two samples fall in the respective category; otherwise, cells are left empty. δD values of the bulk biomass, the methoxyl groups, and the precipitation in the region where the sample was obtained are given in columns 6, 7, and 8, respectively. The Online Isotope Precipitation Calculator (OIPC; accessible at <http://www.waterisotopes.org/>), employing the IAEA database and interpolation algorithms developed by *Bowen and Wilkinson* [2002] and refined by *Bowen and Revenaugh* [2003] and *Bowen et al.* [2005], was used to calculate annual δD values of meteoric water from wood sampling sites at the respective surface elevations. n.m., not measured.

more, δD_{bulk} measurements are sometimes problematic since the samples in question can also contain exchangeable water, i.e., water that can exchange with the environment after collecting the sample and before analysis, so that what is measured does not reflect the original water in the biomass.

[28] The strong isotope depletion can be due to either kinetic fractionation in the H_2 formation process, a depleted source substrate, or both. The dependence of δD_{H_2} on combustion efficiency cannot be explained by the source substrate alone, however. Nevertheless, isotope fractionation within various components of organic material is well established [*Schmidt et al.*, 2003]. Recently, a similar δD depletion within the plant itself has been measured on methoxyl groups of pectin and lignin [*Kepler et al.*, 2007; *Vigano et al.*, 2009], and we report here δD determined for the methoxyl groups (Table 3). Indeed, similar and even slightly stronger depletions are observed, and the fractionation constant for methoxyl groups relative to the bulk biomass is $\alpha_{\text{methoxyl-bulk}} = 0.82 \pm 0.02$. The lower 1σ standard deviation shows that $\delta D_{\text{methoxyl}}$ is more closely linked to δD_{bulk} than δD_{H_2} is and furthermore indicates that contamination from exchangeable water in the δD_{bulk} measurement is probably of minor importance. The quality of the $\delta D_{H_2} - \delta D_{\text{methoxyl}}$ correlation, however, is considerably worse than that of the $\delta D_{H_2} - \delta D_{\text{bulk}}$ correlation. This, together with the fact that δD_{H_2} of the effective combustion samples is in most cases actually enriched relative to $\delta D_{\text{methoxyl}}$, indicates that the similar degree of fractionation may be a coincidence. Identifying the source substrate of the H_2 was beyond the scope of this study.

3.7. Relations Between δD in Precipitation, Bulk Biomass, Methoxyl Groups, and Emitted H_2

[29] To establish the relationship between δD of precipitation and the H_2 emitted, we obtained values of δD precipitation from the Online Isotope Precipitation Calculator (OIPC, accessible at <http://www.waterisotopes.org/>; see caption of Table 3 for more details), which calculates the isotopic composition as a function of geographic location and altitude above sea level.

[30] Figure 6 shows that the variation of the δD of precipitation, bulk biomass, methoxyl groups, and emitted H_2 is related to latitude. All signals show a roughly similar behavior, indicating that the variation in δD in precipitation at different latitudes is a main driver in determining the δD of H_2 from wood burning. The isotopic composition of the bulk biomass is slightly depleted relative to the water, and both methoxyl groups and H_2 from wood burning are strongly depleted.

[31] Figure 7 shows the correlation plot between δD_{H_2} and δD contents of precipitation. Again, there is a considerable degree of scatter, but the correlation slope of 1.03 ± 0.24 is equal to unity within the error bars. Thus, the hypothesis formulated in the beginning is supported by the results. There is a clear relation between δD_{H_2} from wood burning and δD_{H_2O} in precipitation, which probably also holds for other types of biomasses. From the (modeled, OIPC) precipitation data and the δD source signatures determined for each combustion experiment, we can determine a pseudo-fractionation factor between precipitation water and the H_2 produced in the combustion process: $\alpha_{\text{bb-H}_2\text{-precip}} = 0.80 \pm$

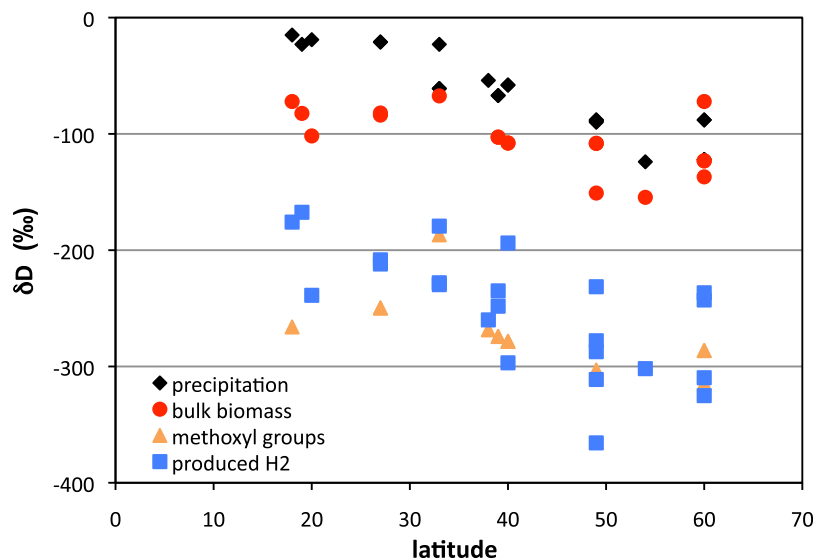


Figure 6. Variation of δD in precipitation, bulk biomass, methoxyl groups, and H_2 produced during combustion. All signatures show a similar behavior.

0.04. Since data on δD in precipitation are readily available, this parameterization could be implemented in global models to more realistically describe δD_{H_2} from biomass burning.

3.8. Comparison to the Literature

[32] The latitude dependence of the isotope source signatures as determined in this study confirms a key assumption from both prior studies [Gerst and Quay, 2001; Rhee *et al.*, 2006b]. However, whereas the δD source signatures can become considerably more enriched than the global average value of $\delta D = -290\text{‰}$ given by Gerst and Quay [2001] for tropical wood burning, none of the fires yielded a source signature as high as $\delta D = -90\text{‰}$, the value postulated by Rhee *et al.* [2006b] for the global average. It is

unlikely that evaporative enrichment of leaves and grasses (see below) can be large enough to account for the difference. The key assumption that does not seem to be valid is the inverse correlation between δD_{bb} and $[H_2]/[CO]$ as presented in Figure 4a of Rhee *et al.* [2006b], a correlation that is not confirmed by our measurements. On the other hand, the good agreement between $\alpha_{H_2\text{-biomass}} = 0.85 \pm 0.05$ determined here for wood samples from various regions and the value found by Gerst and Quay [2001] supports their global average source signature.

[33] In this project, to obtain multiyear-averaged values, we have concentrated on wood samples of trunks or branches that were at least several years old. However, because trees grow with different rates in the different seasons, the results may be biased toward the main growing season.

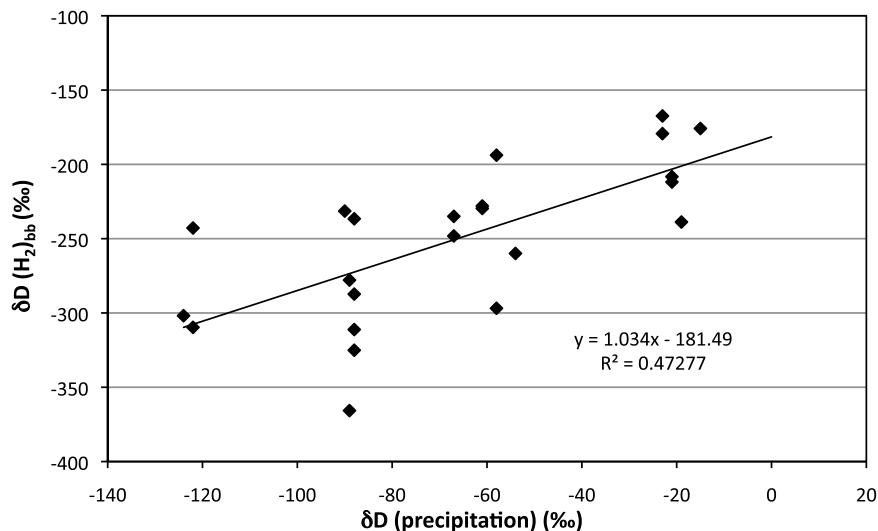


Figure 7. Correlation between $\delta D(H_2)$ produced from wood burning and δD of the precipitation in the growing region.

Also, the δD in precipitation shows a seasonal cycle at many locations. In real natural fires, the principal fuels for the fire are often grasses, leaves, and branches. Those sources are generally isotopically enriched relative to the wood material because evapotranspiration increases δD values in leaves and grasses [Roden and Ehleringer, 2000]. Furthermore, this seasonal biomass is in many regions mostly affected by precipitation in the growing season. Although such effects may have interfered with the influence of precipitation in our study, they will also contribute to the atmospheric signals. For example, if a large fraction of the evaporatively enriched foliage burns in natural wildfires, they may lead to H_2 that is isotopically heavier relative to the values found here for wood samples. More studies need to be carried out to investigate further this effect on evaporative enrichment. In this respect, it is not clear why in the study of Gerst and Quay [2001] fires of pine needles emitted isotopically lighter H_2 than did fires of the branches. Because our experiments were carried out with wood samples, the values presented here may not be adequate for savannah fires, but they should be representative for residential heating or cooking in regions where wood is used.

4. Conclusions

[34] The isotopic composition of H_2 from wood burning was investigated in controlled burning experiments. The results increase the previously available data set (2 experiments, 6 samples in total) by more than an order of magnitude (23 experiments, 152 samples analyzed). Furthermore, wood samples were investigated from locations scattered all over the globe.

[35] Results demonstrate that δD of H_2 is closely related to combustion efficiency. δD decreases with decreasing combustion efficiency, which means that the isotope effects increase in more incomplete combustion, as expected.

[36] Second, δD is generally lower for wood samples that grew at high latitudes than for those from low latitudes. This reflects the latitude gradient of δD in precipitation. As expected, the δD in water from precipitation influences the deuterium isotope ratio of hydrogen in the wood through water taken up by the biomass during growth. When the wood is burned, the spatial distribution of δD in precipitation is found back in the δD of H_2 . A pseudofractionation factor between precipitation water and δD_{H_2} of $\alpha_{H_2-precip} = 0.80 \pm 0.04$ has been derived, which can be implemented in global models to more realistically describe δD_{H_2} from biomass burning.

[37] The water content of biomass has at most a small effect on δD values of H_2 emitted during combustion, indicating that the biomass itself is the major source substrate for H_2 formation.

[38] A similar dependency on δD in precipitation and thus latitude is predicted for all biogenic hydrogen-containing gases, which ultimately originate from plant matter that receive local rainwater [Vigano et al., 2010]. Important examples are CH_4 from biomass burning but also from other sources such as wetlands or ruminants. The potential effect of such a dependency for global isotope models should be investigated, but the effects also need to be verified experimentally.

[39] **Acknowledgments.** We thank our colleagues and friends Tuula Aalto, Martin Vollmer, Michela Maione, Igor Arduini, Christian Wirth, Fiona Scarff, Sander Houweling, Constanza Gómez, John E. Mak, Tracey Evans, Pedro Campuzano Jost, Olga Mayol-Bracero, and Doug Worthy for providing wood samples from different regions of the world. We are indebted to Ivan Vigano, who prepared the samples for bulk and methoxyl group isotope analysis. We thank Carl A. M. Brenninkmeijer for suggesting the possible role of moisture content that sparked the related experiments. The authors greatly appreciate the help of Gregor Feig, who classified the wood samples from Southern Africa. The project was funded by the seventh framework EU project EUROHYDROS and the Dutch Science Foundation NWO (project H_2 budget, 816.01.001). A.G.W., G.H., S.G., and U. P. acknowledge support from the Max Planck Society (MPG) and from the German Research Foundation (DFG, PO1013/2-1).

References

- Andreae, M. O., and P. Merlet (2001), Emission of trace gases and aerosols from biomass burning, *Global Biogeochem. Cycles*, *15*(4), 955–966, doi:10.1029/2000GB001382.
- Bowen, G. J., and J. Revenaugh (2003), Interpolating the isotopic composition of modern meteoric precipitation, *Water Resour. Res.*, *39*(10), 1299, doi:10.1029/2003WR002086.
- Bowen, G. J., and B. Wilkinson (2002), Spatial distribution of delta O-18 in meteoric precipitation, *Geology*, *30*(4), 315–318.
- Bowen, G. J., L. I. Wassenaar, and K. A. Hobson (2005), Global application of stable hydrogen and oxygen isotopes to wildlife forensics, *Oecologia*, *143*(3), 337–348.
- Brand, W. A., et al. (2009), Comprehensive inter-laboratory calibration of reference materials for delta O-18 versus VSMOW using various online high-temperature conversion techniques, *Rap. Commun. Mass Spectrom.*, *23*(7), 999–1019.
- Brenninkmeijer, C. A. M., et al. (2003), Isotope effects in the chemistry of atmospheric trace gases, *Chem. Rev.*, *103*(12), 5125–5162.
- Ehhalt, D. H., and F. Rohrer (2009), The tropospheric cycle of H_2 : A critical review, *Tellus, Ser. B*, *61*(3), 500–535.
- Feck, T., J. U. Grooss, and M. Riese (2008), Sensitivity of Arctic ozone loss to stratospheric H_2O , *Geophys. Res. Lett.*, *35*(1), L01803, doi:10.1029/2007GL031334.
- Feilberg, K. L., M. S. Johnson, A. Bacak, T. Röckmann, and C. J. Nielsen (2007), Relative tropospheric photolysis rates of HCHO and HCDO measured at the European photoreactor facility, *J. Phys. Chem. A*, *111*(37), 9034–9046.
- Gehre, M., H. Geilmann, J. Richter, R. A. Werner, and W. A. Brand (2004), Continuous flow $^2H/^1H$ and $^{18}O/^{16}O$ analysis of water samples with dual inlet precision, *Rap. Commun. Mass Spectrom.*, *18*(22), 2650–2660.
- Gerst, S., and P. Quay (2001), Deuterium component of the global molecular hydrogen cycle, *J. Geophys. Res.*, *106*(D5), 5021–5031, doi:10.1029/2000JD900593.
- Greule, M., A. Mosandl, J. T. G. Hamilton, and F. Keppler (2008), A rapid and precise method for determination of D/H ratios of plant methoxyl groups, *Rap. Commun. Mass Spectrom.*, *22*(24), 3983–3988.
- Johnson, M. S., K. L. Feilberg, P. von Hessberg, and O. J. Nielsen (2002), Isotopic processes in atmospheric chemistry, *Chem. Soc. Rev.*, *31*(6), 313–323.
- Keppler, F., et al. (2007), Stable hydrogen isotope ratios of lignin methoxyl groups as a paleoclimate proxy and constraint of the geographical origin of wood, *New Phytol.*, *176*(3), 600–609.
- Lobert, J. M., D. H. Scharffe, W. M. Hao, and P. J. Crutzen (1990), Importance of biomass burning in the atmospheric budgets of nitrogen-containing gases, *Nature*, *346*(6284), 552–554.
- Lobert, J. M., et al. (1991), Experimental evaluation of biomass burning emissions: Nitrogen and carbon containing compounds, edited by J. S. Levine, pp. 133–142, MIT Press, Cambridge, Mass.
- Novelli, P. C., et al. (1999), Molecular hydrogen in the troposphere: Global distribution and budget, *J. Geophys. Res.*, *104*(D23), 30,427–30,444, doi:10.1029/1999JD900788.
- Pieterse, G., M. C. Krol, and T. Röckmann (2009), A consistent molecular hydrogen isotope chemistry scheme based on an independent bond approximation, *Atmos. Chem. Phys.*, *9*(21), 8503–8529.
- Price, H., et al. (2007), Global budget of molecular hydrogen and its deuterium content: Constraints from ground station, cruise, and aircraft observations, *J. Geophys. Res.*, *112*(D22), D22108, doi:10.1029/2006JD008152.
- Rahn, T., J. M. Eiler, N. Kitchen, J. E. Fessenden, and J. T. Randerson (2002a), Concentration and dD of molecular hydrogen in boreal forests: Ecosystem-scale systematics of atmospheric H_2 , *Geophys. Res. Lett.*, *29*(18), 1888, doi:10.1029/2002GL015118.

- Rahn, T., N. Kitchen, and J. M. Eiler (2002b), D/H ratios of atmospheric H_2 in urban air: Results using new methods for analysis of nano-molar H_2 samples, *Geochim. Cosmochim. Acta*, *66*(14), 2475–2481.
- Rahn, T., et al. (2003), Extreme deuterium enrichment in stratospheric hydrogen and the global atmospheric budget of H_2 , *Nature*, *424*(6951), 918–921.
- Rhee, T. S., J. E. Mak, C. A. M. Brenninkmeijer, and T. Röckmann (2004), Continuous-flow isotope analysis of the D/H ratio in atmospheric hydrogen, *Rap. Commun. Mass Spectrom.*, *18*, 299–306.
- Rhee, T. S., C. A. M. Brenninkmeijer, M. Brass, and C. Brühl (2006a), Isotopic composition of H_2 from CH_4 oxidation in the stratosphere and the troposphere, *J. Geophys. Res.*, *111*(D23), D23303, doi:10.1029/2005JD006760.
- Rhee, T. S., C. A. M. Brenninkmeijer, and T. Röckmann (2006b), The overwhelming role of soils in the global atmospheric hydrogen cycle, *Atmos. Chem. Phys.*, *6*, 1611–1625.
- Rhee, T. S., C. A. M. Brenninkmeijer, and T. Röckmann (2008), Hydrogen isotope fractionation in the photolysis of formaldehyde, *Atm. Chem. Phys.*, *8*, 1353–1366.
- Rice, A., P. D. Quay, J. Stutsman, R. Gammon, H. Price, and L. Jaeglé (2010), Meridional distribution of molecular hydrogen and its deuterium content in the atmosphere, *J. Geophys. Res.*, *115*, D12306, doi:10.1029/2009JD012529.
- Röckmann, T., T. S. Rhee, and A. Engel (2003), Heavy hydrogen in the stratosphere, *Atmos. Chem. Phys.*, *3*, 2015–2023.
- Röckmann, T., et al. (2010), Isotope effect in the formation of H_2 from H_2CO studied at the atmospheric simulation chamber SAPHIR, *Atmos. Chem. Phys.*, *10*, 5343–5357.
- Roden, J. S., and J. R. Ehleringer (2000), Hydrogen and oxygen isotope ratios of tree ring cellulose for field-grown riparian trees, *Oecologia*, *123*(4), 481–489.
- Sander, S. P., et al. (2006), Chemical Kinetics and Photochemical Data for Use in Atmospheric Studies, Evaluation Number 15, Tech. rep., Jet Propulsion Laboratory, Pasadena.
- Schmidt, H.-L., R. A. Werner, and W. Eisenreich (2003), Systematics of 2H patterns in natural compounds and its importance for the elucidation of biosynthetic pathways, *Phytochem. Rev.*, *2*, 61–85.
- Schultz, M. G., T. Diehl, G. P. Brasseur, and W. Zittel (2003), Air pollution and climate-forcing impacts of a global hydrogen economy, *Science*, *302*(5645), 624–627.
- Tromp, T. K., R.-L. Shia, M. Allen, J. M. Eiler, and Y. L. Yung (2003), Potential environmental impact of a hydrogen economy on the stratosphere, *Science*, *300*, 1740–1742.
- Vigano, I., et al. (2009), The stable isotope signature of methane emitted from plant material under UV irradiation, *Atmos. Environ.*, *43*(35), 5637–5646, doi:10.1016/j.atmosenv.2009.5607.5046.
- Vigano, I., et al. (2010), Water drives the deuterium content of the methane emitted from plants, *Geochim. Cosmochim. Acta*, *74*, 3865–3873.
- Vollmer, M. K., S. Walter, S. W. Bond, S. P. Soltic, and T. Röckmann (2010), Molecular hydrogen (H_2) emissions and their isotopic signatures (H/D) from a motor vehicle: Implications on atmospheric H_2 , *Atmos. Chem. Phys.*, *10*, 3021–3051.
- Warwick, N. J., S. Bekki, E. G. Nisbet, and J. A. Pyle (2004), Impact of a hydrogen economy on the stratosphere and troposphere studied in a 2-D model, *Geophys. Res. Lett.*, *31*(5), L05107, doi:10.1029/2003GL019224.
- Werner, R. A., B. A. Brunch, and W. A. Brand (1999), Conflo III—An interface for high precision $\delta^{13}C$ and $\delta^{15}N$ analysis with an extended dynamic range, *Rap. Commun. Mass Spectrom.*, *13*, 1–5.
- Yapp, C. J., and S. Epstein (1982), Climatic significance of the hydrogen isotope ratios in tree cellulose, *Nature*, *297*, 636–639.
-
- W. A. Brand, Max Planck Institute for Biogeochemistry, Joh.-Joachim-Becher-Weg 27, 55128 Jena, Germany.
- C. X. Gómez Álvarez, T. Röckmann, C. van der Veen, and S. Walter, Institute for Marine and Atmospheric Research Utrecht, Utrecht University, Princetonplein 5, 3508CC Utrecht, Netherlands.
- M. Greule, S. S. Gunthe, G. Helas, F. Keppler, U. Pöschl, and A. G. Wollny, Max Planck Institute for Chemistry, Hans-Knöll-Str. 10, 07745 Mainz, Germany.